



# Benchmarking Snow Fields of ERA5-Land in the Northern Regions of North America

Robert Sarpong<sup>1</sup>, Ali Nazemi<sup>1</sup>

<sup>1</sup> Department of Building, Civil and Environmental Engineering, Concordia University, Montreal, H3G 1M8, Canada

*Correspondence to:* Ali Nazemi (ali.nazemi@concordia.ca)

**Abstract.** Reanalysis products provide new opportunities for assessments of historical Earth System states. This is crucial for snow variables, where ground-based observations are sparse and incomplete, and remote sensing measurements still face limitation. However, because reanalysis data are model-based, their accuracy must be evaluated before being applied in impact and attribution studies. In this study, we assess the accuracy of ERA5-Land's snow cover, snow depth, and Snow Water Equivalent (SWE) across monthly, seasonal, and annual scales, within the ecological regions of Canada and Alaska, regions that are characterized by prolonged seasonal snow cover. Using MODIS satellite snow cover observations and the gridded snow depth/SWE analysis data from the Canadian Meteorological Centre, we conduct a consistent benchmarking of ERA5-Land's snow fields to (1) identify discrepancies at both gridded and regional scales, (2) evaluate the reproducibility of spatial structure of snow variables, and (3) uncover potential spatial patterns of discrepancies in ERA5-Land's snow statistics. Our results highlight significant discrepancies, particularly for snow depth and SWE, where ERA5-Land tends to grossly overestimate long-term mean values and interannual variability, while underestimating trends, i.e., moderating positive trends and exaggerating negative ones. The discrepancies in SWE, however, are primarily driven by biases in snow depth rather than snow density. Therefore, we advise against the direct use of ERA5-Land's snow depth and SWE in Canada and Alaska. While snow cover and snow density may still be useful for impact and attribution studies, they should be applied with caution and potential bias corrections particularly at local and smaller scales.

## 1 Introduction

Snow plays a vital role in regulating the Earth's climate and hydrological systems. Most notably, snowpack is crucial for water resource management as it acts as a natural freshwater reservoir, storing water during cold seasons and releasing it in warmer months, when water is most needed (Bair et al., 2016; Deng et al., 2019). In addition, snow strongly influences the Earth's surface albedo, impacting the surface energy budget (Lackner et al., 2022; Willeit and Ganopolski, 2018). It also serves as a natural thermal insulator, protecting soil from extreme temperatures (Kim et al., 2018; You et al., 2014). Understanding snow dynamics is therefore essential for assessing water availability, regional climate patterns, ecosystem health, and human activities, particularly in high-latitude and high-elevation areas (Sexstone et al., 2016; Stiegler et al., 2016; Mitterer and Schweizer, 2013). This knowledge has become even more pressing as climate change accelerates the decline in snow cover



and disrupts regional water and energy balances (e.g., Barnett et al., 2005; Huning and Aghakouchak, 2020; Musselman et al., 2021; Fang and Leung, 2023; Ryberg, 2024).

From a hydrological perspective, the extents of Snow Cover (SC), Snow Depth (SD), and Snow Water Equivalent (SWE) offer crucial insights into regional climate and water resource management (Wang and Zheng, 2020; Li et al., 2017). SC refers to  
35 the fraction of the land area covered by snow at a given time, which is essential for understanding albedo and, consequently, land-atmosphere interactions (Callaghan et al., 2011; Lehning, 2013). SD, which measures the vertical distance from the ground to the top of the snowpack, is a fundamental variable for estimating water availability and plays a critical role in disaster management within snow-dominated regions (Shijin et al., 2022; Kazama et al., 2008). SWE quantifies the amount of water stored in the snowpack, serving as a key parameter for managing water resources, hydropower, and flood risks (Skaugen et al., 2012; Vionnet et al., 2021). These snow variables, exhibit significant spatial and temporal variability, driven by factors  
40 such as latitude, topography, land cover, and weather patterns (Stiegler et al., 2016; Bormann et al., 2013).

Understanding and monitoring these dynamics are crucial for effective land and water management, as well as for anticipating the impacts of climate change. While in-situ snow measurements provide the most direct and accurate data on snow variables (Stähli et al., 2004; Brown et al., 2021; Vionnet et al., 2021), such data are often temporally and spatially limited, and collecting  
45 them is labour-intensive and costly (Kouki et al., 2023). Satellite remote sensing offers a valuable alternative for snow monitoring, providing a synoptic view across large areas (Dietz et al., 2012; Broxton and van Leeuwen, 2020). However, it also faces limitations (Brubaker et al., 2005; Appel, 2018). For instance, temporal coverage can be limited and inconsistent (Hassler and Lauer, 2021). In addition, while remote sensing SC is relatively straightforward using optical sensors (Hall and Riggs, 2007), estimating SD and SWE remains challenging (Dong et al., 2005; Schilling et al., 2024). Passive microwave  
50 sensors, such as the Advanced Microwave Scanning Radiometer for Earth Observing System (AMSR-E; Kelly et al., 2003) and the Special Sensor Microwave/Imager (SSM/I; Grody and Basist, 1996) are commonly used for SD and SWE estimates but tend to lose accuracy in areas with deep snow or complex terrain (Foster et al., 2005; Byun and Choi, 2014). Active sensors like Light Detection and Ranging (LiDAR; Deems et al., 2013) and radar (Marshall and Koh, 2008) can enhance accuracy, but their temporal coverage is limited and they are not available globally. Even for SC, challenges remain due to factors such as  
55 cloud cover, vegetation interference, and polar nights, hindering snow detection in certain regions (Molotch et al., 2004; Hall et al., 1998; Trepte et al., 2003).

Recently, climate reanalysis data have emerged for understanding historical Earth System states (Lindsay et al., 2014). In essence, reanalysis is a scientific approach that merges historical climate and land observations with simulations of Earth System models to produce a comprehensive, consistent, and continuous record of the Earth's atmosphere, oceans, and land  
60 surface over an extended period. These datasets also include snow-related variables, allowing assessments of long-term trends and variability across broad spatial and temporal scales. However, reanalysis data remain model-dependent and can exhibit biases, particularly in regions where observational data are sparse (Graham et al., 2019; Sun et al., 2018). As a result, numerous



studies have intercompared reanalysis products and benchmarked them against observations to evaluate their accuracy, consistency, and applicability for different uses (Morice et al., 2012; Rapaic et al., 2015; Schumacher et al., 2020). Despite providing important insights, these intercomparison studies face a number of limitations. One key issue is the scale mismatch between the grid resolution of reanalysis data and the point-based nature of in-situ observations. This mismatch is often overlooked (Hamm et al., 2020; Xu et al., 2022; Fatolahzadeh Gheysari et al., 2024), including for the validation of snow-related variables (Orsolini et al., 2019; Baxter et al., 2024; Ma et al., 2023). Although some exceptions exist (Kouki et al., 2023; Monteiro and Morin, 2023), this oversight can hinder the assessment of the spatial representation of snow characteristics in reanalysis data. To address this, downscaling methods are suggested to reconcile the coarse resolution of reanalysis data with finer-scale observations (Kusch and Davy, 2022). However, downscaling introduces its own uncertainties, and in some cases, upscaling or regridding data to a common resolution may be a more suitable approach, especially for larger domains (Lei et al., 2023; Kouki et al., 2023). Furthermore, many benchmarking studies focus primarily on gridded or regional intercomparisons (Henn et al., 2018; Monteiro and Morin, 2023; Scherrer et al., 2023), often neglecting to assess how well spatial structure of snow characteristics are captured or whether there are spatial patterns in discrepancies. This can obscure systematic errors and biases in reanalysis products and may lead to inappropriate applications in decision-making contexts.

Given the aforementioned limitations, the primary objective of this study is to benchmark the SC, SD, and SWE variables from the fifth generation of the European Centre for Medium-Range Weather Forecasts (ECMWF) Land Reanalysis (ERA5-Land; Muñoz-Sabater et al., 2021) over northern North America, specified here by Canada and Alaska. This large region, covering nearly 12 million km<sup>2</sup> (~9% of the global landmass), is heavily influenced by prolonged seasonal snow cover, which profoundly shapes its climate, water availability, land characteristics, ecosystems, and human activities (Boelman et al., 2019; Callaghan et al., 2011; DeBeer et al., 2016). The snow processes across Canada and Alaska exhibit considerable variability in time and space, driven by factors such as seasonality, climate tele-connectivity, latitude, elevation, proximity to large water bodies, and land cover (Bitz and Battisti, 1999; Brown, 2010; Bormann et al., 2013; Nazemi et al., 2017). For example, while substantial snow accumulation occurs in the Canadian Rockies, and interior Alaska, snow depth is relatively shallow in coastal British Columbia.

ERA5-Land is land-focused and offers a finer spatial resolution than its global counterpart, ERA5 (Hersbach et al., 2020); however, unlike ERA5, it does not assimilate land-surface variables, and apply ERA5 forcing for offline land simulations at finer scales. Previous global assessments and regional benchmarking studies have highlighted that ERA5-Land tends to overestimate snow variables, especially in mountainous areas (Orsolini et al., 2019; Kouki et al., 2023; Monteiro and Morin, 2023; Akyurek et al., 2023); however, these overestimations may partly result from scale discrepancies (Lei et al., 2023). In addition, ERA5-Land's snow density over China has shown good agreement with ground-truth observations (Gao et al., 2022). These findings raise three critical questions: (1) How would ERA5-Land's snow variables perform when benchmarked against reference datasets at a consistent scale? (2) Can ERA5-Land replicate the spatial structure observed in reference data, and is



95 there any spatial structure in the discrepancies? (3) What is the role of snow density in potential biases of SWE? To pursue these questions, we apply a consistent benchmarking framework using a number of statistics across the 21 ecological regions of Canada and Alaska. We use reference satellite observations from the Moderate Resolution Imaging Spectroradiometer (MODIS; Hall et al., 2002) for benchmarking SC. For SD and SWE, we rely on the Canadian Meteorological Centre's (CMC's) snow analysis, which integrates observed and modelled snow depth with estimates of snow density used for calculation of SWE (Sturm et al., 2010). The CMC's SD/SWE product is widely regarded as one of the most accurate gridded datasets for North America and has been extensively used as a reference in benchmarking studies (Frei et al., 2005; Niu and Yang, 2007; Brown and Frei, 2007; Cooper et al., 2018; Yoon et al., 2022).

## 2 Data and methods

### 2.1 Snow data

105 ERA5-Land (hereafter ERA5L) is a high-resolution reanalysis dataset, produced to capture land processes with a greater precision at the hourly scale and 0.1° grid scale from 1st January 1950 to present. The data consist of simulation results based on the Hydrology-Tiled ECMWF Scheme for Surface Exchanges over Land model (HTESSEL; Balsamo et al., 2009). The model enhances the representation of land surface processes by incorporating advanced treatments of snow hydrology, soil-vegetation interactions, and energy fluxes. For a brief expansion of how SD, SC, and SWE of ERA5L are represented and modelled by the HTESSEL model, see Section S1 of the Supplement. These snow variables are tested against reference products, introduced below. SD, SC and SWE data of ERA5L at their native temporal and spatial resolutions are obtained globally for the period of January 1st 1950 to December 31st 2023 using the ECMWF Climate Data Store Application Programming Interface (CDS-API) – see Data availability.

CMC's SD/SWE product is used here as reference data for benchmarking corresponding variables of ERA5L. CMC provides daily analysed SD and monthly estimated SWE from 1998 to 2020 over the northern hemisphere at 24 km grid scales. The snow depth analysis is performed using in-situ daily snow depth observations, and interpolation with “first-guess” estimates, generated by a simple snowpack model. The snowpack model is forced with analysed temperatures and forecast precipitation from the Canadian forecast model. In-situ observations include snow depths from surface synoptic observations and other reports from the World Meteorological Organization (WMO) information system. For details of the analysis see Brown et al. (2003). For a brief outline of the procedure with which SD and SWE estimates are produced, see Section S2 of the Supplement. The CMC's daily SD and monthly SWE data are downloaded for the entire data period of August 1st 1998 to December 31st 2020 at their native spatial resolution from National Aeronautics and Space Administration's (NASA) Snow and Ice Data Centre (NSIDC) using the HyperText Transfer Protocol Secure (HTTPS) links. Note that monthly SWE data are missing



within all grids of the data domain during months July, August and September. We have also masked out regions with  
 125 unrealistically high SD and SWE values according to developers' recommendation – see Data availability.

The MODIS's SC data are widely used in climate monitoring, hydrological modelling, and snowpack assessments (e.g.,  
 Saavedra et al., 2018; Parajka and Blöschl, 2008; Dong, 2018; Di Marco et al., 2021). Here, we use MODIS global monthly  
 Level-3 (L3) snow cover data to benchmark ERA5L's SC product. This version of MODIS provides a composite data by  
 monthly averaging of the daily SC observations of the MODIS/Terra Daily L3 Global 0.05Deg CMG (MOD10C1), with the  
 130 goal of monitoring and analysing snow extent (Hall et al., 2002; Maurer et al., 2003). For a brief explanation of MODIS's SC  
 algorithm, see Section S3 of the Supplement. The MODIS monthly snow cover are downloaded from 1 March 2000 to 31  
 December 2023 at its native spatial resolution 5 km from NASA's NSIDC using the HTTPS links – see Data availability.

## 2.2 Elevation data

As the properties of snowpack significantly alters with elevation, we obtain the Global Multi-resolution Terrain Elevation Data  
 135 2010 (GMTED2010; Danielson and Gesch, 2011) to monitor changes in SD, SC and SWE with respect to altitude.  
 GMTED2010 is an advanced digital elevation model (DEM) dataset produced by the U.S. Geological Survey (USGS) and the  
 National Geospatial-Intelligence Agency (NGA). GMTED2010 combines multiple elevation data sources and is widely used  
 in applications such as hydrological modelling, climate research, geospatial analysis, and environmental monitoring, and  
 disaster risk management due to its higher resolution and improved data quality (see e.g., Pakoksung and Takagi, 2021;  
 140 Ermolaev et al., 2017; Amatulli et al., 2018). The data provides various topographical variables from 84°N to 56°S across  
 multiple resolutions (~250, ~500 and ~1000 m). Here we consider mean elevation data at 1 km. The data is publicly available  
 through USGS – see Data availability.

## 2.3 Data harmonization

Table 1 summarizes our data support. As each dataset has its own data coverage and spatiotemporal scale, a harmonization is  
 145 necessary. We first consider the common data period of 1 March 2000 to 31 December 2020 and clip the data over the landmass  
 of Canada and Alaska using shapefiles available at Global Administrative Areas (GADM; <https://gadm.org/data.html>). We  
 then upscale the hourly and daily data to monthly in their native spatial grids by simple temporal averaging. This is done for  
 all data except elevation data as well as CMC's SWE and MODIS' SC data that are already at a monthly scale. We then  
 spatially upscale the monthly data to ~25 km grid cells, except for CMC data that are already in a comparable resolution. The  
 150 spatial upscaling is done by the weighted area averaging. The weight for each grid is assigned based on the percentage of the  
 original grid area that is located inside the larger ~25 km grid cell. Through the upscaling, we also handle the missing data. If  
 the data is missing in one or more smaller grids, the upscaled data is also considered as missing. This is a harsh filter and  
 particularly affects upscaling of ERA5L grids adjacent to coastlines and waterbodies as upscaling may require considering  
 grids that are not within the land mask of ERA5L. However, it ensures data consistency and benchmarking power.



155 **Table 1.** Data support and they role in this study along with their native temporal and spatial scales, and period of data coverage

Product name	Role	Variable name	Data period	Temporal scale	Spatial scale
ERA5-Land	Test data	Snow depth (SD)	1950 – 2023	Hourly	~9 km
		Snow cover (SC)			
		Snow water equivalent (SWE)			
CMC	Reference data	Snow depth (SD)	1998 – 2020	Daily	24 km
		Snow water equivalent (SWE)		Monthly	
MODIS	Reference data	Snow cover (SC)	2000 – 2023	Monthly	5 km
GMTED2010	Complementary data	Mean elevation	N/A	N/A	~1 km

While after rescaling, the data are in similar grids sizes, they do not perfectly match. To precisely match the grids, we regridded all the rescaled data on a common 25 km grid cells. We use the grid system implemented in NASA’s Making Earth System Data Records for Use in Research Environments (MEaSUREs) data for the global landscape FT Earth System Data Record (FT-ESDR; Kim et al., 2017). The regridding is done by the  $k$ -nearest neighbour interpolation. In a nutshell,  $k$ -nearest neighbour is a non-parametric method for estimating a variable in an unknown point based on its known values in the neighbouring points that are weighted based on the inverse Euclidian distance (Hatami and Nazemi, 2021, 2022). We use four nearest neighbours for the interpolation across all datasets.

After regridding, we pair the test and reference data for each snow variable, and consider only those grids in which both test and reference data have no missing data during the benchmarking period of 2000 to 2020. We also temporally upscale the data from monthly to seasonal and annual. We consider months October, November, December as fall, January, February and March as winter, and April, May, June as spring. As CMC’s SWE data are missing in July, August and September, we exclude these three months from our study and consider the remaining nine months for bringing the data into the annual scale.

### 3 Case study and benchmarking procedure

170 To better understand the variability in snow variables and how they are compared between ERA5L and reference products, we consider benchmarking ERA5L’s SD, SC and SWE across 21 ecological regions that cover this domain of Canada and Alaska. In brief, ecological regions are part of a hierarchical classification system that divides North America into areas with similar geology, climate, vegetation and ecosystem (Omenrik, 2004; Wright et al. 1998; McMahon et al., 2004). This classification systems facilitates consistent view at different geographic areas (see Omernik and Griffith, 2014). From north to south, these



175 ecological regions include (1) Artic Cordillera, (2) Northern Arctic, (3) Alaska Tundra, (4) Brooks Range Tundra, (5) Southern  
 Artic, (6) Alaska Boreal Interior, (7) Taiga Cordillera, (8) Taiga Plain, (9) Taiga Sheild, (10) Hudson plain, (11) Softwood  
 shield, (12) Mixed Wood Shield, (13) Atlantic Highlands, (14) Boreal plain, (15) Boreal Cordillera, (16) Western Cordillera,  
 (17) Mixed Wood plains, (18) Temperate Prairies, (19) West Central Semiarid Prairies, (20) Marine West Coast Forest, and  
 (21) Cold Deserts. Figure 1(a) shows these regions and uniquely colour codes them. These colour codes and the above  
 180 numerical ordering are used in the rest of the paper to refer to different regions. With an area of ~1.5 million km<sup>2</sup>, Northern  
 Arctic (ecological region 2) is the largest region, while the ~50,000 km<sup>2</sup> Cold Deserts (ecological region 21) is the smallest.  
 Figure 1(b) shows the elevation of the harmonized ERA5L grids over the domain, revealing the elevation variation between  
 [0 3400] m at the 25 km spatial scale. Figure 1(c) shows the percentage of grids in each ecological region used for  
 benchmarking at the annual scale. As can be seen many grids are not considered for analysis of SC in the northern regions,  
 185 particularly in Arctic Cordillera and Brooks Range Tundra that have no data. This is due to the fact that MODIS's SC data is  
 missing in these regions in the winter months due to polar nights. Also, only around 20% of the grids in Atlantic Highlands  
 are considered. This is due to the particular upscaling applied here, which causes many grids with proximity to water bodies  
 are eliminated. On average, 58%, 86% and 78% of grids in each region are considered for annual analyses of SC, SD and  
 SWE, respectively. Figure 1(d) shows the percentage of grids in the entire domain that are considered at the annual, seasonal  
 190 and monthly scales. Depending on the variable and the period, between 58% to 87% of grids participate in the benchmarking.

For the purpose of benchmarking a given snow variable in an ecological region, we consider four characteristics, namely long-  
 term mean, standard deviation, trend and autocorrelation, and calculate them at every grid and across annual, seasonal and  
 monthly scales using both ERA5L and corresponding reference data. Long-term mean represents the climatological average  
 for the considered variable. Standard deviation measures interannual variability and quantifies the dispersion around the long-  
 195 term mean. The higher the standard deviation is, the more variability exists in the data. Trend signifies monotonic changes in  
 the data during the benchmarking period. We quantify the trend using Mann-Kendall's test with Sen's slope (see Amir Jabbari  
 and Nazemi, 2019; Zaerpour et al., 2021a) and consider  $p$ -values of 0.05 or lower as the thresholds for significance of trend.  
 Autocorrelation helps understanding the persistence and existence of memory in the data. We start with lag-0 and increase the  
 lag time by one until the  $p$ -values exceeds 0.05. We consider the lag before the break as the effective memory.

200 After these statistics are calculated for a given snow variable in a grid cell using both ERA5L and reference products, we  
 quantify the discrepancy either using simple or relative differences:

$$D = X_{ERA5L} - X_{Reference} \quad (1)$$

$$RD = \frac{X_{ERA5L} - X_{Reference}}{X_{Reference}} \times 100 \quad (2)$$

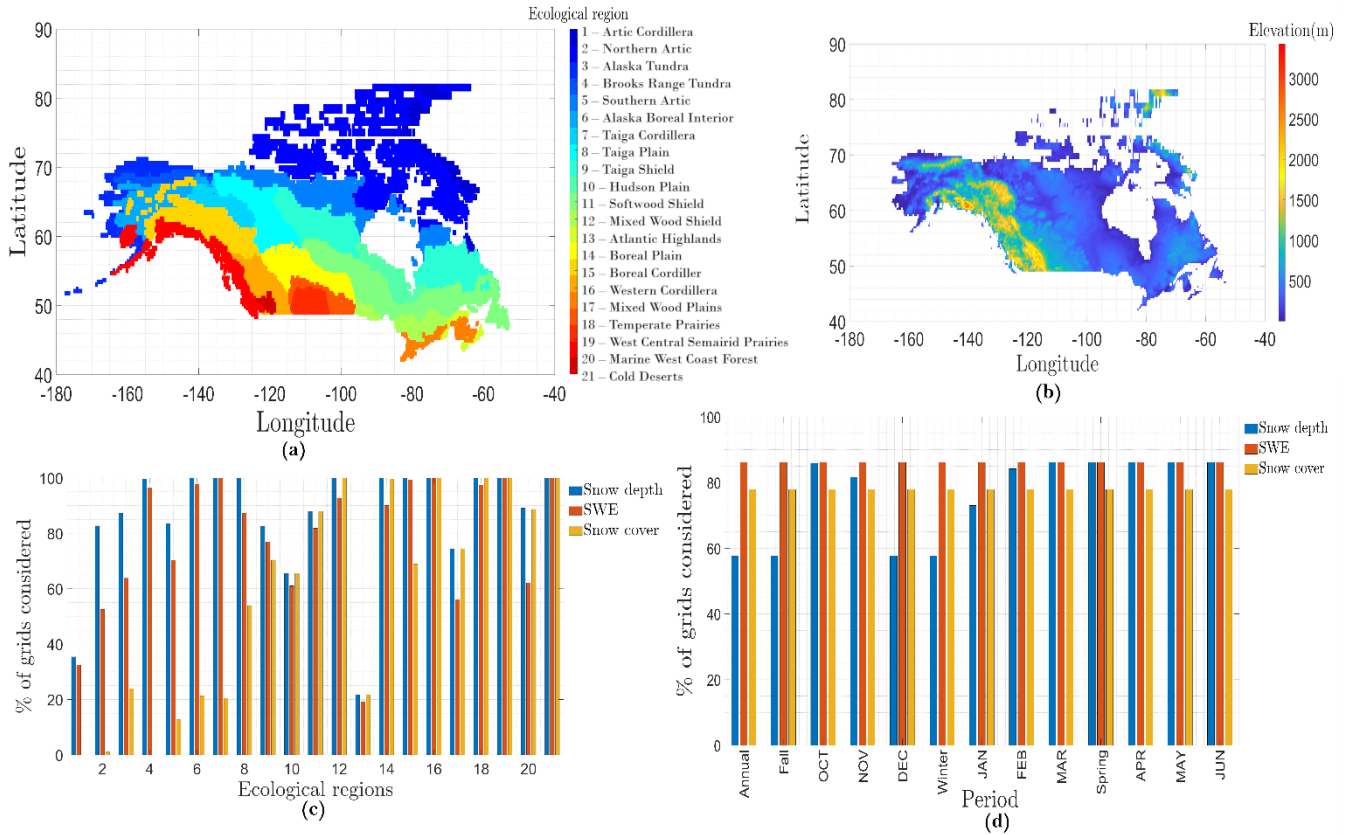


**Figure 1: (a) Spatial extent of the 21 ecological regions in Canada and Alaska; (b) variability in elevation across Canada and Alaska based on harmonized elevation at the 25 km spatial scale; (c) the ratios of grids in each ecological regions that are used for annual intercomparison of ERA5-Land snow variables, i.e., snow depth, Snow Water Equivalent (SWE), and snow cover, with reference products; and (d) temporal variations in the ratios of grids across Canada and Alaska, used for intercomparing ERA5-Land snow variable with reference products.**

In which  $D$  and  $RD$  are simples and relative differences, and  $X_{ERA5L}$  and  $X_{Reference}$  are the statistics derived by ERA5L and corresponding reference product, respectively. Note that  $D$  follows the unit of the statistics considered, however  $RD$  is in percentage. As  $RD$  can be large, we also consider a scaled version of  $RD$  using the following logarithmic transformation:

$$RD^* = \begin{cases} \log(RD) & RD > 1\% \\ 0 & -1\% \leq RD \leq 1\% \\ -\log(|RD|) & RD < -1\% \end{cases} \quad (3)$$



In which  $RD^*$  is the scaled  $RD$ . We also consider quantifying the spatial dependence between statistics (as well as the discrepancies in the estimates of the statistics) with latitude, longitude and elevation at each ecological region to identify whether the considered statistics obtained from ERA5L and the reference product displays a similar spatial structure or not. When the spatial dependence is calculated for discrepancies, it highlights whether there is a systematic spatial structure in the discrepancies in the considered ecological region. We use non-parametric Kendall's tau (Zaerpour et al., 2021b; Kaemo et al., 2022) for quantifying the spatial dependencies with latitude, longitude and elevation.  $p$ -values of 0.05 and lower are considered for identifying the significant spatial dependencies.

## 4 Results

Below we evaluate (1) gridded discrepancies; (2) regional discrepancies; and (3) discrepancies in spatial structures of ERA5L snow variables and corresponding reference products. We look into these discrepancies at annual, seasonal and monthly scales. For the sake of brevity, figures related to discrepancies at the seasonal and annual scales are provided in the Supplement.

### 4.1 Discrepancies at the grid scale

Using Empirical Cumulative Distribution Functions (ECDFs), we evaluate gridded discrepancies between ERA5L snow variables and reference products within each ecological region at the annual scale. Within each ecological region and for a given snow variable, we estimate the four annual characteristics, i.e., long-term mean, standard deviation, trend, and effective memory, across all the grids using the ERA5L and associated reference products. We then quantify the discrepancies between pair statistics, and establish ECDFs of the estimated discrepancies at each ecological region. Figure 2 summarizes the results. Rows and columns are related to snow variables and considered statistics, respectively. From left to right, columns refer to long-term mean, standard deviation, trend and the effective memory derived from autocorrelation test. In each panel, ECDFs of the 21 regions are represented by different colours according to the legend. Discrepancies in the long-term mean, standard deviation and trend, are quantified by  $RD^*$ ; whereas  $D$  is used for autocorrelation memory. This analysis reveals the tendency of ERA5L in each region toward under- or overestimating the statistics inferred from reference products. The tendency toward under or overestimation can be deduced by looking at whether the median discrepancy in each region (i.e.,  $ECDF=0.5$ ) stays on the left or right side of the dashed line, respectively.

While ERA5L tends to overestimates the gridded long-term mean of MODIS's SC in 10 regions, mainly located in the south, it underestimates the standard deviation of MODIS's SC in 15 out of 19 ecological regions. The tendency to underestimate MODIS statistics is also seen for trends (17 ecological regions). When it comes to autocorrelation memory, ERA5L captures the autocorrelation estimates of MODIS in the majority of grids across all ecological regions. However, in those grids that the discrepancy occurs, it only tends toward underestimation.

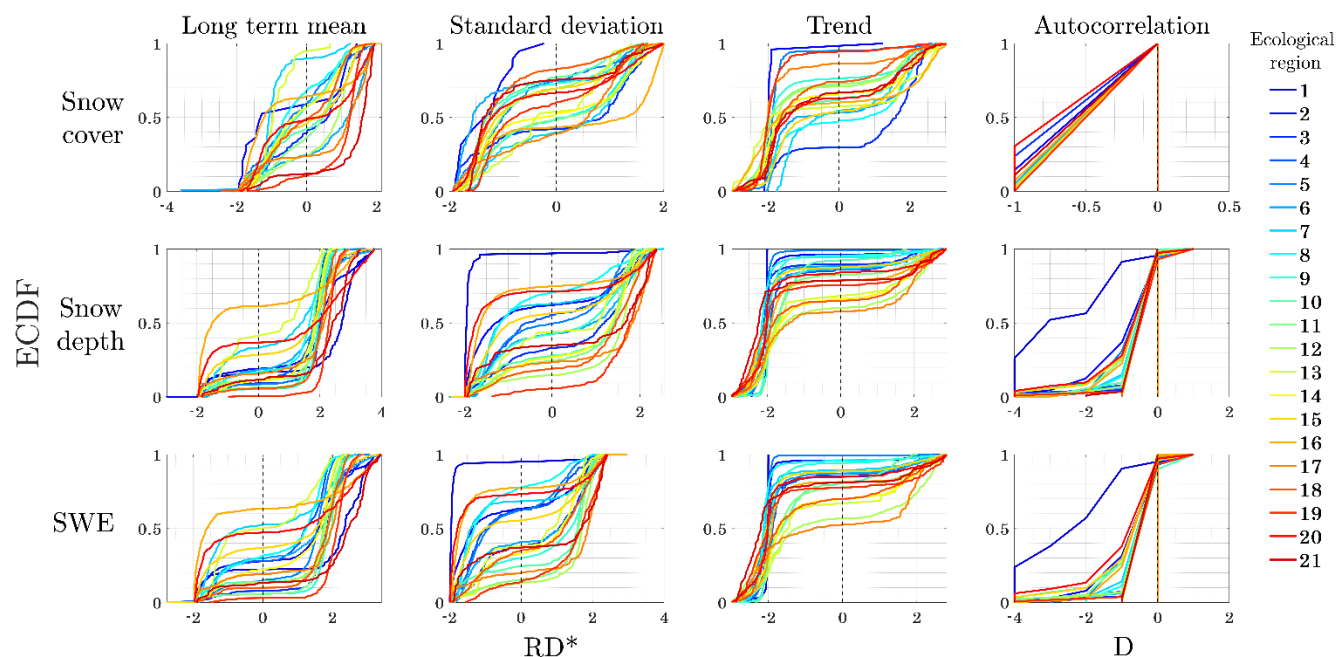


**Figure 2: Empirical Cumulative Distribution Functions (ECDFs) representing gridded discrepancies between statistical characteristics of ERA5-Land and reference products for snow cover (top row), snow depth (middle row) and Snow Water Equivalent (SWE; bottom row) at the annual scale.**

ERA5L overestimates the long-term mean of CMC's SD and SWE in almost all ecological regions (20 in the case of SD; 18 in the case SWE) and these overestimations can be grossly large in some grids in multiple ecological regions (up to nearly 100 times). Although more moderately, ERA5L also overestimates standard deviation of CMC's SD and SWE (12 out of 21 ecological regions for both variable). Having said that in some regions, e.g., Artic Cordillera, the variability in annual SD is underestimated by ERA5L in nearly all grids. Despite the tendency to overestimation of trend and standard deviation, the trends in annual SD and SWE are significantly underestimated by the ERA5L across all ecological regions. It should be noted that in the case of negative trends, these underestimations mean steeper negative Sen's slope derived by ERA5L. While the tendency of ERA5L to underestimate the autocorrelation memory of SD and SWE is much less, it is still more severe than the one related to SC.

We repeat this analysis at the seasonal and monthly time scales. Figure S1 in the Supplement summarizes our findings. In each panel, boxplots show the percentage of grids across 21 regions in which ERA5L statistics overestimate corresponding values of the reference products. To provide a means for comparison, the first greyed boxplot in each panel is related to the annual scale; and red, blue, and green boxplots respectively show the results for the fall, winter, and spring seasons and months.



The solid black line in each panel shows the expected seasonal and monthly number of grids across the 21 ecological regions in which ERA5L overestimates the reference product. Looking at SC, the tendency for overestimating the long-term mean of MODIS is more in the fall and spring season, particularly during October and May. Having said that during the core snow season, the tendency of ERA5L for overestimating the MODIS's long-term mean declines. Overall, it is expected that ERA5L overestimates MODIS's annual long-term mean in ~48% of grids. This ratio alters seasonally between 45% (winter) to 48% (fall). The range of discrepancies increases at the monthly scale and stays between 30% (January) to 70% (May). Similar conclusions can be drawn regarding the standard deviation and trend estimates of SC obtained by ERA5L; however, the issue of underestimation is more pronounced for these two statistics. Our results emphasize that ERA5L underestimate the winter's monthly trends in SC in almost all grids across Canada and Alaska. When it comes to autocorrelation memory, the chance of overestimation decreases in all ecological regions, however, it relatively increases during the winter, particularly in February. Similar to the annual scale, discrepancies in statistics of SD and SWE are similar across seasonal and monthly scales. For both variables, the expected percentage of grids that overestimate CMC's long-term mean stays well above 50%, except for SWE in June. For standard deviation and trend, the chance of overestimating CMC's statistics inclines in fall and declines in winter months; although the chance of overestimation is much lower in the case of trend than standard deviation and expected values stay well below 50% across all seasons and months. The chance of overestimation significantly declines in the case of autocorrelation memory. Despite similarities in discrepancies of SD and SWE for the four considered statistics, there are some differences as well, which can be due to discrepancies in snow density. This will be discussed in Section 5.2.

## 4.2 Discrepancies at the regional scale

Here we explore the expected values and variabilities of discrepancies between ERA5L and reference products across 21 ecological regions. Figure 3 summarizes the result at the annual scale. In each panel,  $x$  and  $y$  axes measure the expected value and variability of discrepancies between ERA5L and reference products in a given ecological region. Each dot corresponds to one of the ecological regions based on the colour code shown in the legend and its coordinates are the first and second moments of the associated ECDFs in Figure 2. Note that for annual long-term mean, standard deviation and trend, first and second moments of RD's are shown; however, for autocorrelation memory, moments are related to the simple difference (Eq. 1). Considering long-term mean of SC, ERA5L demonstrate an expected discrepancy of  $\pm 10\%$  between ERA5L and MODIS in 13 out of 19 ecological regions. While in 7 regions, ERA5L overestimates MODIS statistic, it underestimates in 10 and provide a zero discrepancy in 2 ecological regions. In 10 out of 19 regions, the Coefficient of Variations (CVs) of discrepancies ( $CV = \frac{\text{standard deviation}}{\text{mean}}$ ) stays below 1, indicating more consistent gridded discrepancies between ERA5L and MODIS estimates across the ecological region. Considering the standard deviation of SC, in 16 ecological regions the MODIS statistics are underestimated by ERA5L and this underestimation is 10% and more in 10 ecological regions. Also, in 11 out of 19 ecological regions the CV is above 1, indicating high relative variability, and the fact that gridded discrepancies are dispersed around the expected value in these ecological regions. Similar results can be seen with respect to trend, in which ERA5L underestimate

trends inferred from MODIS in 15 out of 19 ecological regions; and the rate of underestimation is more 10% in 14 regions. 11 out of 19 ecological regions have CV below 1, indicating consistent gridded discrepancies in these regions. Expected mean and variability of regional discrepancies between ERA5L and MODIS largely decline for autocorrelation memory, which stay on or below -0.1 in 15 out of 19 of ecological regions.

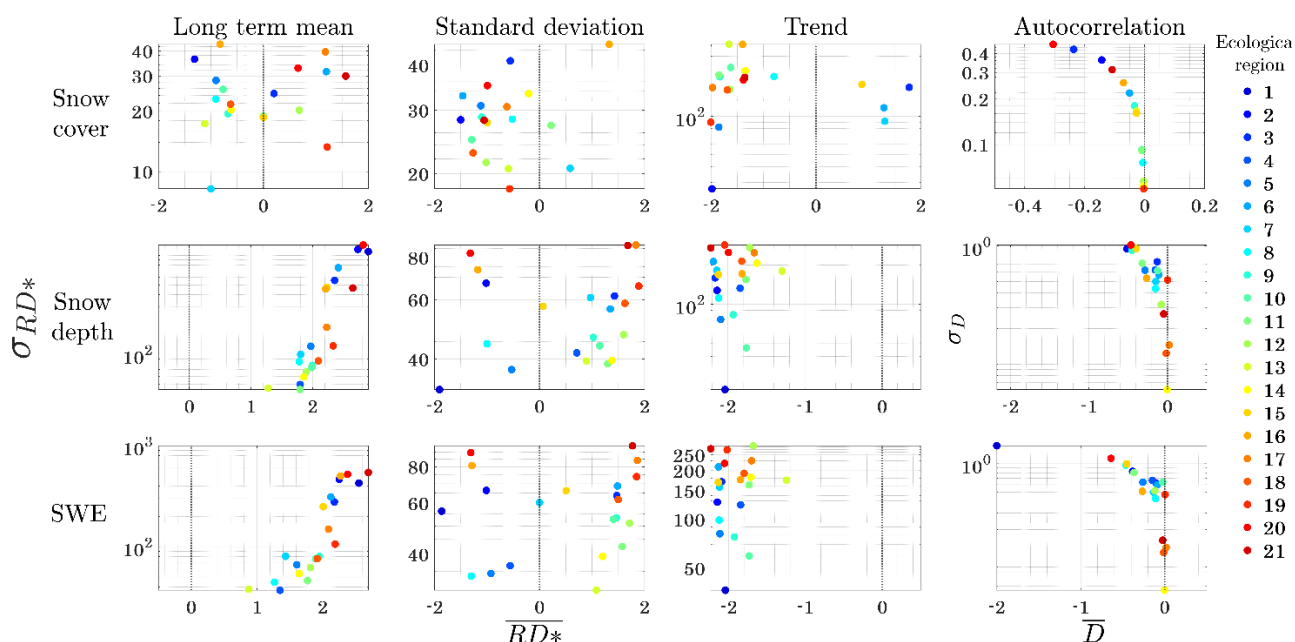


**Figure 3: First and second moments of annual discrepancies between ERA5-Land and reference products across ecological regions of Canada and Alaska in (from left to right) long-term mean, standard deviation, trend and lag memory of snow cover (top row), snow depth (middle row) and Snow Water Equivalent (SWE; bottom row)**

Regional discrepancies in characteristics of SD and SWE are comparable. Long-term mean for both SD and SWE are consistently overestimated by ERA5L across all ecological regions and the rate of overestimation can be large (up to 8.5 time of CMC). In 13 out of 21 ecological regions, the CVs for discrepancies in long-term mean stay below 1, indicating consistent gridded overestimation within these ecological regions. Interannual variability, quantified by standard deviation, is also overestimated in majority of ecological regions (15 ecological regions in the case of SD and 13 ecological regions in the case of SWE) and the rate of overestimation can be as large as the inferred CMC statistics in some southern ecological regions. The CVs of discrepancies stay above 1 in 11 out of 21 regions, meaning less consistent gridded discrepancies within these ecological regions. Despite overestimating long-term mean and standard deviation, ERA5L consistently underestimate the trend in regional SD and SWE across all ecological regions and the rate of underestimation can be as large as the estimated trend by CMC. With respect to the autocorrelation memory in annual SD and SWE series, much better match between ERA5L



and CMC are observed across all regions except in the case of SWE in the Northern Arctic, in which both the first and second  
 310 moment of discrepancies can be considerably larger than other ecological regions.

We also look at the expected values of the first and second moments of discrepancies at seasonal and monthly scales across  
 all 21 ecological regions. Figure S2 in the Supplement summarizes our findings. In each panel, dark and light grey lines  
 correspond to the expected values for the first and second moments of discrepancies that are gauged by the left and right y  
 axes. Considering the long-term mean and standard deviation of SC, the expected first and second moments of discrepancies  
 315 decline during the winter and incline in fall and spring. During the winter season and months, the ERA5L has the tendency to  
 underestimate MODIS statistics; however, it tends to overestimate MODIS during fall and spring. Regarding trends in SC,  
 expected mean of seasonal discrepancies are considerably lower than the monthly values. Expected means of discrepancies in  
 trends of SC increase at the monthly scale, particularly in winter months (underestimating). Considering the autocorrelation  
 memory of SC, the expected first and second moments of discrepancies tend toward zero, except in February. Moving to SD  
 320 and SWE, the expected first and second moments of discrepancies in long-term mean and standard deviation decline during  
 the winter. While the overall tendency of ERA5L is to overestimate CMC's standard deviation, it can underestimate the  
 variability inferred by CMC in March. Similar discussion can be extended to trend in SD and SWE. While the overall tendency  
 of ERA5L is to underestimate the CMC's trend, it overestimates CMC's statistics in May.

#### 4.3 Discrepancies in spatial structures of snow variables

325 To inspect the preservation of spatial structure in snow characteristics, we explore the spatial dependencies of snow  
 characteristics inferred from ERA5L and reference products with longitude, latitude and elevation. We note that there can be  
 four states, revealing the degree of similarity/dissimilarity between spatial structures obtained from ERA5L and reference  
 products. The first state is the condition in which the spatial dependencies obtained by ERA5L and reference products have  
 the same sign and significance level. This condition reveals strong similarity in the spatial structures and coded here by (1,1).  
 330 The second condition is the condition in which the signs of spatial dependence inferred by ERA5L and reference products are  
 the same, but the significance level is different. This condition portrays weaker similarity between the spatial structure inferred  
 by competing products and is coded by (1,0). The third and fourth conditions reveal differences between the spatial structures  
 and are coded by (0,1) and (0,0) respectively. (0,1) states the condition in which the sign of spatial dependence obtained by  
 competing products are different, but the significance levels are the same. (0,0) states a condition in which both signs and  
 335 significance of dependence between competing products are different. Figure 4 summarizes the results related to annual  
 characteristics. In each panel, we identify the four states of dependence with longitude, latitude and elevation across the 21  
 ecological regions using light grey, dark grey and black step lines respectively.

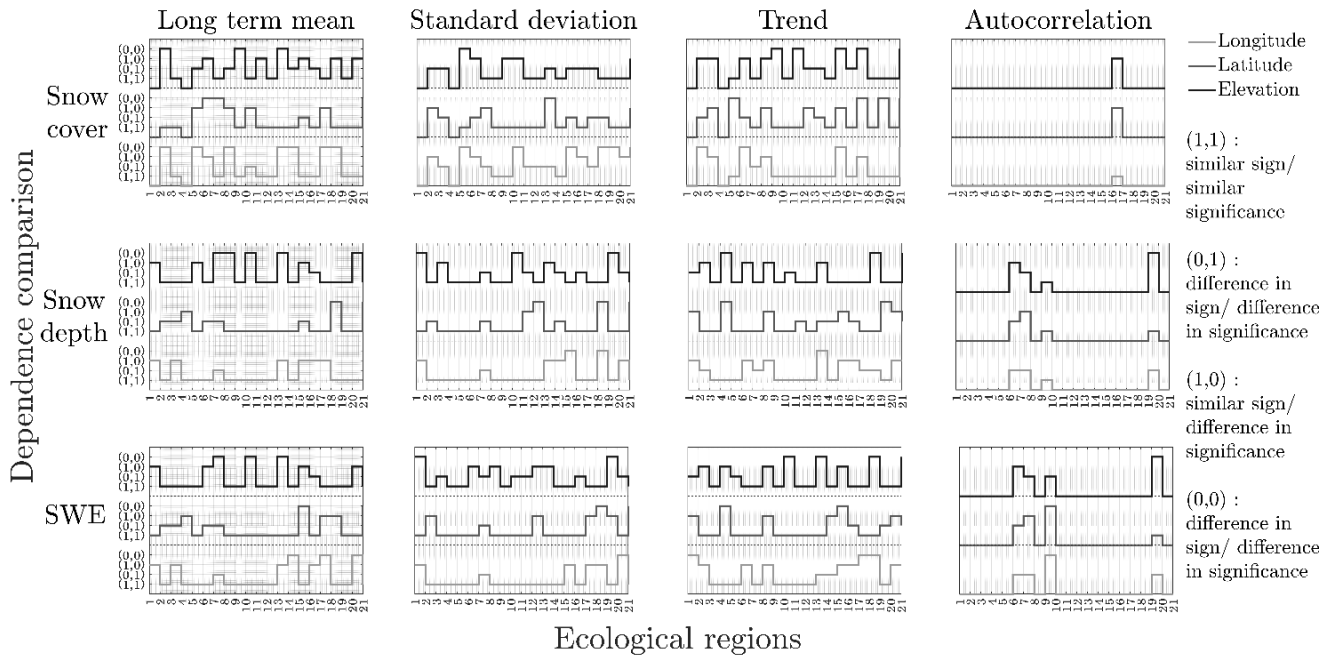


**Figure 4: Comparison between spatial structures in annual snow variables obtained by ERA5-Land and the reference products across the 21 ecological regions. The spatial structures are proxied by the dependencies between snow characteristics (i.e., long-term mean, standard deviation, trend, and autocorrelation memory) and longitude, latitude and elevation. The comparison is coded by an ordered binary pair, where the first and second digits represent the agreement in the sign and significance of the spatial dependence (1 agree; 0 disagree).**

Considering long-term mean of SC, the ERA5L and MODIS show strong similarity in spatial structure with longitude, latitude, and elevation in 9, 11 and 6 ecological regions, respectively. For standard deviation of SC, strong similarity in spatial structures is observed in 3, 10 and 8 regions with respect to longitude, latitude, and elevation respectively. Regarding the trend of SC, 11, 8 and 7 regions show similar spatial structures with respect to longitude, latitude, and elevation respectively. For autocorrelation memory, it should be noted that in all ecological regions except Western Cordillera (ecoregion 16), there is not a revealing spatial structure with both ERA5L and MODIS as majority of grids exhibit lag-0 autocorrelation. In Western Cordillera, strong similarity in spatial structure of ERA5L and MODIS only observed with respect to longitude.

For long-term mean of SD, the ERA5L and CMC exhibit strong similarity in spatial structure with longitude, latitude, and elevation in 13, 13 and 11 regions, respectively. For standard deviation of SD, strong similarity is observed in 13, 14 and 10 regions with respect to longitude, latitude, and elevation respectively. Regarding the trend of SD, 9, 10 and 12 regions show strong similarity in spatial structures with respect to longitude, latitude, and elevation. Similar condition as noted for SC is also for autocorrelation memory of SD as in the majority of ecological region, there is no memory retrieved for SD from ERA5L and/or CMC and again the only meaningful autocorrelation is lag-0 in majority of the grids. However, in those



ecological regions where there is a spatial structure, only in 1, 2 and 1 ecological regions ERA5L and CMC show strong similarity in spatial structure with respect to longitude, latitude and elevation.

With respect to long-term mean of SWE, the ERA5L and CMC exhibit strong similarity in spatial structure with longitude, latitude, and elevation in 13, 12, and 13 ecological regions respectively. With respect to standard deviation of SWE, strong similarity in spatial structures is observed in 15, 14 and 9 ecological regions with respect to longitude, latitude, and elevation respectively. Regarding the trend of SWE, 9, 12 and 11 ecological regions exhibit strong similarity in spatial structures with respect to longitude, latitude, and elevation respectively. Again, in the majority of ecological region, there is no spatial structure for autocorrelation memory of SWE retrieved from ERA5L and/or CMC and the only meaningful autocorrelation memory is lag-0 in majority of the grids. In those ecological regions where a spatial structure can be retrieved for autocorrelation memory, only 1 region depicts strong similarity with respect to latitude.

We also consider evaluating the spatial dependencies at seasonal and monthly scales. Figure S3 in the Supplement summarizes our findings in terms of percentage of ecological regions that exhibit similar spatial structures between (1) long-term mean, (2) standard deviation, (3) trend, and (4) autocorrelation memory with respect to longitude (black bars), latitude (dark grey bars) and elevation (light grey bars). Considering all snow variables and across all temporal scales considered, only long-term mean exhibit possibility for the strong similarity in spatial structure longitude, latitude, and elevation. For all other snow characteristics and across all time scales, only possibilities for strong similarity in spatial structures are with elevation. The highest percentage of similarity between ERA5L and CMC is in the dependence of long-term mean of SWE with latitude inferred for October, which is similar in 16 ecological regions. These findings are largely in contrast with what observed in the annual scale (Fig. 5), and highlights the potential for large divergences between spatial structures across monthly and seasonal scales, despite more alignment at the annual scale.

## 5 Discussion

The findings presented in Section 4 evaluates the gridded, regional and spatial discrepancies of ERA5L with reference products across different annual, seasonal and monthly scales. One essential question remained unanswered is whether there is any spatial structure within the discrepancies identified. In addition, while we highlight similarities between discrepancies of ERA5L and CMC with regard to SD and SWE characteristics, we also note certain differences that may be related to discrepancies in estimates of snow density, necessitating further analyses. In this section, we explore these lines of inquiry.

### 5.1 Spatial structure of discrepancies

To explore the spatial structure of annual discrepancies, we look at the Kendall's tau of gridded discrepancies with longitude, latitude and elevation. Figure 5 summarizes our findings. In each panel, the three boxplots refer to Kendall's tau of discrepancies with longitude, latitude and elevation across the 21 ecological regions, sorted from left to right. Dots show the



ecological regions in which the dependency between discrepancies and spatial elements are significant at the  $p$ -values of 0.05 or less. Considering SC, discrepancies between estimates of long-term mean have significant dependencies with longitude, latitude and elevation across 13, 12 and 15 ecological regions, respectively. Discrepancies between interannual variabilities of SC, proxied with standard deviation, have significant spatial dependence in 16, 15 and 10 ecological regions with longitude, latitude and elevation, respectively. Similarly, discrepancies in the estimates of trend in SC demonstrate strong spatial dependencies with longitude, latitude and elevation across 13, 12, and 16 ecological regions, respectively. While discrepancies in autocorrelation memory of SC is much less than those for other three statistics, still the existing discrepancies demonstrate significant spatial dependencies with longitude, latitude and elevation across 6, 6, and 7 regions.

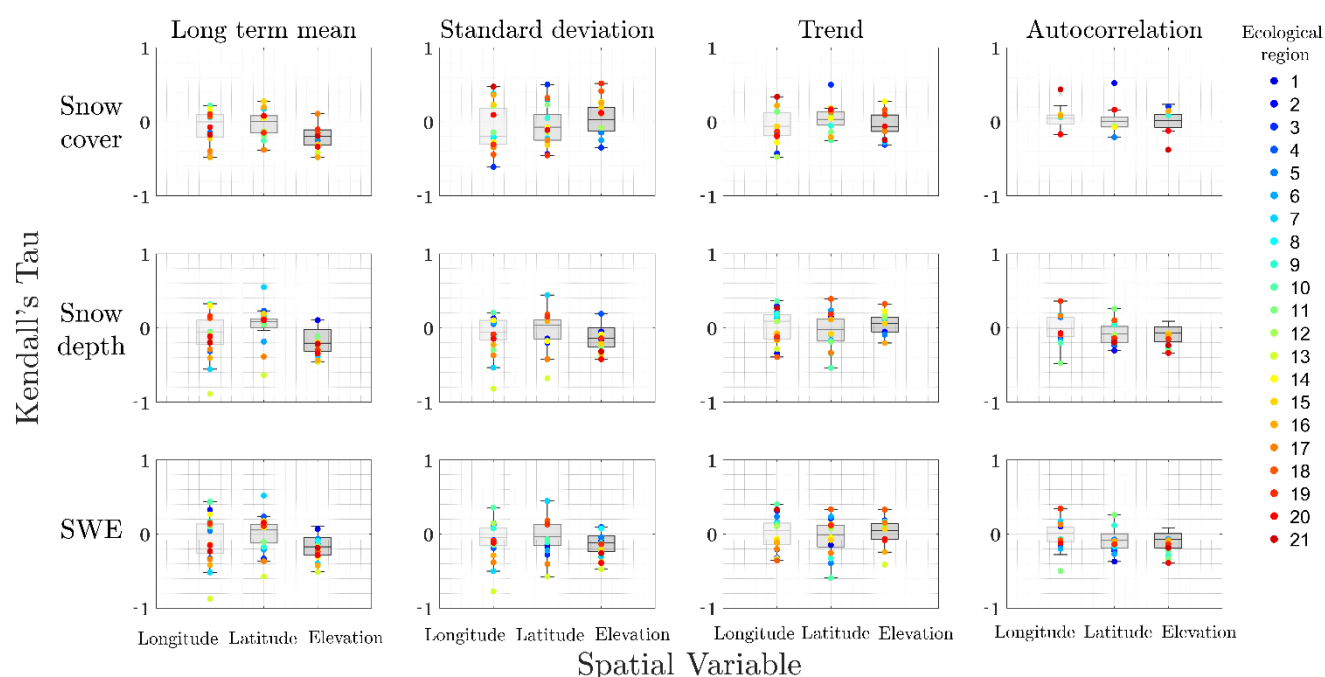


**Figure 5: Spatial structures of discrepancies between ERA5-Land and reference products for annual long-term mean, standard deviation, trend, and autocorrelation memory of snow cover (top row), snow depth (middle row), and Snow Water Equivalent (SWE; bottom row) across 21 ecological regions. Ecological regions in which discrepancies have significant dependencies with longitude, latitude, and elevation, are marked with color dots according to the legend.**

Significant spatial patterns of discrepancies can be also seen in estimates of SD and SWE. Considering long-term mean of SD, significant spatial patterns with longitude, latitude and elevation are observed across 16, 16 and 15 ecological regions, respectively. Strong spatial patterns for discrepancies in long-term mean estimates of SWE are also observed with longitude, latitude and elevation. Regarding discrepancies in estimated standard deviation of SD and SWE, 16 ecological regions show significant spatial pattern, although the location of ecological regions can alter depending on the snow variable and the spatial



405 element considered. With respect to discrepancies in trend estimates of SD and SWE, only 1 and 2 ecological regions do not exhibit strong spatial pattern with longitude, respectively. Trend estimates of SD and SWE demonstrate significant dependence with latitude in 16 ecological regions and with elevation in 13 ecological regions. Similarly, the discrepancies in the autocorrelation memory of SD and SWE have significant dependence with longitude in 11 ecological regions, with latitude in 13 and 12 ecological regions, and with elevation in 10 and 11 ecological regions, respectively.

410 We also look into the spatial patterns of discrepancies across seasonal and monthly scales. Figure S4 in the Supplement summarizes our results. In each panel, the considered temporal scales are ordered in the  $x$  axes. For each temporal scale, the three lines show the interquartile ranges of regional dependencies between discrepancies and longitude (red), latitude (green) and elevation (blue), and the dot on each line shows the expected dependence across the 21 ecological regions. Note that for the autocorrelation memory of SC and SD the spatial dependencies for discrepancies cannot be retrieved in several ecological  
 415 regions as there is not discrepancy between ERAL and reference data.

Our results show strong spatial patterns of discrepancies across all temporal scales. Considering all the grids in Canada and Alaska, the discrepancies in estimates of long-term means of SC show significant dependence with longitude, latitude and elevation in all temporal scales, although the sign of dependence alters across different temporal scales. With respect to the discrepancies in estimates of standard deviation, again significant spatial patterns observed across all temporal scales and  
 420 spatial elements, except for the dependence with longitude in the January and May, as well as the dependence with latitude in fall season. With respect to the discrepancies in trend estimates of SC, the only insignificant spatial patterns are related to dependence with longitude in fall, and with latitude in May. For autocorrelation memory, in all temporal scales in which spatial dependence can be retrieved, it is identified as significant.

Discrepancies in long-term mean of SD and SWE have significant spatial pattern across all temporal scales except with  
 425 longitude in December for SD and with latitude in November for SWE. Discrepancies in standard deviation do not show significant dependencies with longitude in November, December and winter season for SD, and in October for SWE. Discrepancies in the trend of SD do not show significant dependencies with longitude in October and with latitude in fall season and October. For trend in SWE, discrepancies have insignificant dependencies with longitude in October and winter season and with latitude in October. For discrepancies in autocorrelation memory estimates of SD and SWE, the cases with  
 430 insignificant dependencies grows compared to other statistics. For those temporal scales for which the spatial pattern of discrepancies can be retrieved, the insignificant cases include dependencies with elevation in November, January, February and March, as well as with longitude in January and May. For SWE insignificant cases with elevation are in fall and winter, as well as November, December and February. Insignificant cases with longitude include those in winter, January and May. For latitude, the only insignificant case is in May.



## 5.2 The role of snow density across scales

As described in Sections S.1 and S.2, snow density in both ERA5L and CMC are model-based. In order to better understand the nature of discrepancies in SWE estimates between the two products, we look at the estimates of long-term mean and trend of snow density and how they differ ERA5L and CMC. Figure 6 shows the gridded estimates of annual long-term mean (top row) and normalized trend (bottom row) of snow density obtained from the two products along with their corresponding RDs.

Normalized gridded trends are estimated by dividing the Sen's slope to long-term mean at each grid. Major differences in the long-term mean estimates of snow density over Canada and Alaska can be seen. Overall, the ERA5L underestimates long-term mean inferred from CMC in about 80% of the domain, mainly in the interior west, north east and the eastern slope of the Rocky Mountains. ERA5L however overestimate snow density in eastern Canada and parts of north east, in western Alaska, and western slopes of the Rocky Mountains.

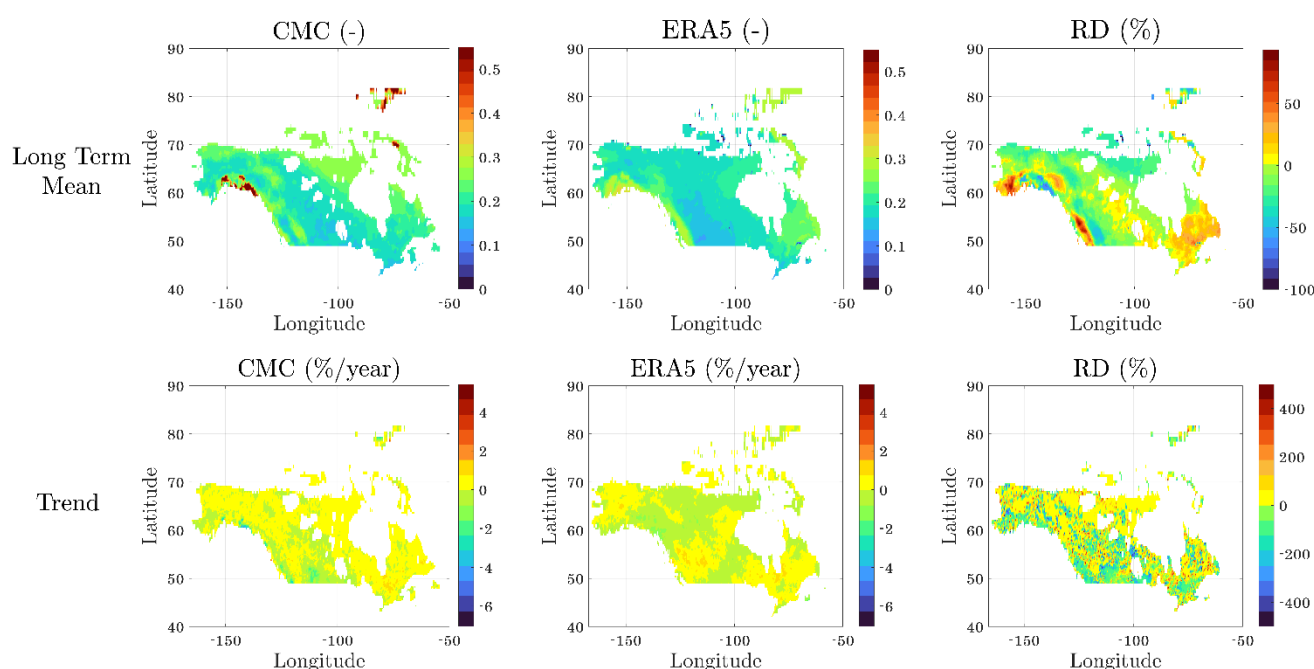


**Figure 6: Spatial variabilities in the annual long-term mean (top) and trend (bottom) of snow-to-water density across Canada and Alaska along with the Relative Discrepancies (RDs) between ERA5-Land and CMC products.**

When it comes to estimated trend in the snow density, CMC exhibits negative trends in around 44% of the grids, out of which ~8% of grids have significant negative trends ( $p$ -value  $\leq 0.05$ ). ERA5L however reveal negative trend in around 46% of grids, out of which 10% show significant negative trend. Generally, ERA5L tends to underestimate the trend in snow density inferred



from CMC. This underestimation means moderated Sen's slope in positive trends and exacerbated Sen's slope in the case of negative trends.

We repeat the above analyses at monthly and seasonal scales. Figure S5 in the Supplement summarizes our results for gridded long-term means (left panel) and normalized trends (right panel) of snow density inferred from CMC (yellow envelope) and ERA5L (green envelope). In each panel, solid lines show the expected estimates by each product across the entire domain. For both long-term mean and the trend, the range of estimates of CMC are considerably larger. In addition, for both products and considering both characteristics, the ranges of estimates increase in spring and decrease in winter, which is intuitively appealing considering the occurrence wet snow due to melt in the spring season. It is expected that ERA5L underestimates the CMC's long-term mean of snow density across Canada and Alaska in majority of temporal scales considered, except in October, May, June, and spring season. Despite significant differences in the inferred ranges of trend, both products provide rather identical expected trends across the whole domain of Canada and Alaska and in all temporal scales considered.

In order to have a better understanding of the discrepancies, we look at the RDs in long-term means and trends in each ecological region and inspect whether there are any dependencies with elevation. Figure 7 summarizes our finding, in which top and bottom rows are related to long-term mean and trend in snow density respectively. Boxplots in left panels show the gridded RDs and the red solid lines highlight the expected discrepancies across the 21 ecological regions. The middle panels show the scatter plots of gridded RDs against elevation. The data related to each ecological region are uniquely color-coded and black solid lines show the best linear fit to all the grids in the domain. Right panels depict the dependencies between gridded RDs and elevation across the 21 ecological regions. Coloured bars in each panel represent the ecological regions in which the dependencies are significant.

Considering the expected values of RDs related to long-term mean, the results reveal expected underestimations of ERA5L across 13 ecological regions. There is an obvious north to south gradient in discrepancies, where in northern ecological regions ERA5L tends to underestimate CMC's long-term snow density, whereas the tendency is toward overestimating CMC's long-term mean across southern ecological regions. The expected range of discrepancies is between -29% (Arctic Cordillera) to 26% (Cold Deserts). Note that the range of gridded discrepancies can be much larger, i.e., from 100% underestimation in Arctic Cordillera to 96% overestimation in Maritime West Coast Forest. The most frequent underestimation is seen in Taiga Cordillera, where ERA5L underestimates the long-term snow density in 97% of grids. In contrast, ERA5L overestimates CMC's long-term mean in 84% of grids in Cold Deserts. Looking at the best line fitted to the scatterplot of RDs in long-term mean against elevation, it is clear that the rate of underestimation increases at higher elevations. In fact, there is no chance for positive RDs at elevations above 2100 meters. Increasing the rate of underestimation with elevation is also valid across 18 ecological regions, from which 12 regions show significant Kendall's tau. Only in 3 ecological regions, i.e., northern Arctic, Taiga Shield and Softwood Shield, there are significant positive dependencies between gridded RDs and elevation showing that the rate of underestimation declines (or the rate of overestimation increases) as elevation increases.

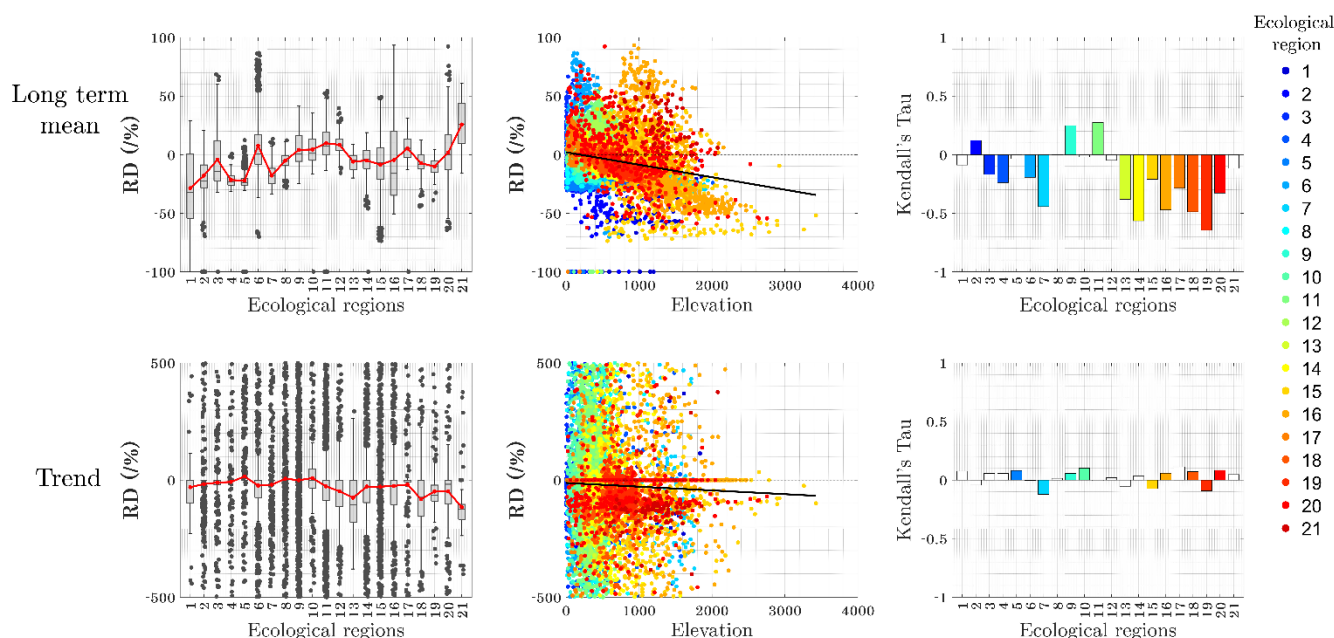


**Figure 7: (Left column) gridded discrepancies in the annual mean (top) and trend (bottom) of snow-to-water density across 21 ecological regions in Canada and Alaska. Expected discrepancies are shown by solid red lines; (middle column) variation in gridded discrepancies of the long-term mean (top) and trend (bottom) of snow-to-water density with respect to elevation, colour coded for each ecological region. The solid black lines show the best linear fit; (right column) the spatial dependence between discrepancies in the long-term mean (top) and trend (bottom) of snow-to-water density with elevation across 21 ecological regions. Colour bars show regions with significant Kendall's tau.**

490 Considering the gridded trend in snow density, large over- and underestimation can be seen by ERA5L across all ecological regions. Having said that, in most of the ecological regions the grids with large over- and underestimations cancel the effect of one another and the expected dependencies across each ecozone are much less significant than the gridded values. While in northern regions, the expected discrepancies is close to zero, the tendency to underestimating the CMC's snow density increases in southern ecological regions. The most frequent underestimation is seen in Cold Deserts, in which CMC's trends

495 in snow density are underestimated in 88% of grids. In contrast, the most frequent overestimation is seen in Alaska Boreal Interior, in which ERA5L overestimates CMC's trend in snow density in 42% of grids. Similar to long-term mean, when all the grids in the domain are considered, the rate of underestimation in CMC's trend in snow density grows by increasing elevation; however, the rate of the incline is greatly moderated in the case of trend compared to long-term mean. This conclusion is subject to large regional variations and is confirmed in only in 3 ecological regions that show significant negative

500 dependencies between RDs of gridded trends and elevation.



We also look at the gridded RDs across other temporal scales and explore how they change with respect to elevation. Figure S6 in the Supplement summarizes our findings, in which top and bottom rows are related to discrepancies with respect to long-term mean and trend in snow density, respectively. Left panels show the range of RDs in the entire Canada and Alaska and across different temporal scales, in which the solid black lines show the expected RDs. Middle panels show the linear evolution of discrepancies with elevation across different temporal scales. The grey lines are related to the annual scale, shown in Fig S5. Solid and dashed red, blue and green lines show the linear change of RDs with elevation across fall, winter, and spring seasons and months respectively (see the legend for the symbology). The right panels show the range of regional dependencies between RDs and elevation, measured by Kendall's tau, at different temporal scales. The solid black lines show the expected Kendall's tau across all the 21 ecological regions. Considering the long-term mean, the range of discrepancies significantly increases in spring and decreases in winter, October and January. The overall tendency of ERA5L is to underestimate the CMC's snow density, expect in the spring and May. Similar to the annual scale, the ERA5L tends to underestimate the CMC's snow density more as the elevation increases; however, this tendency is subject to temporal variations. During winter and fall the slope of the fitted lines are moderated compared to the annual scale, whereas in the spring season and months, steeper inclines in underestimation are observed with elevation. Analysis of ecozonal dependencies of RDs in long term mean of snow density with elevation show expected negative Kendall's taus across the 21 ecological regions, which confirms the increase in the rate of underestimation at higher elevations.

Considering the gridded RDs in trend of snow density, large over- and underestimation are observed across all temporal scales, however, the ranges of RDs are reduced during winter and in March. While the overall tendency of ERA5L is to underestimate the trend in snow density inferred by CMC, it is also expected that ERA5L slightly overestimates the trend in CMC's snow density during winter and spring seasons, particularly in March. The rate of underestimation of the CMC's trend increases in higher elevations, particularly during spring and June. The regional dependencies between RDs in trend and elevation also approves this, as across the expected regional dependencies between RDs and elevation are negative across all monthly and seasonal scales, except November.

## 6 Summary, conclusion and further remarks

Reanalysis products offer new opportunities for conducting consistent and comprehensive assessments of historical Earth System variables across the atmosphere, land, and oceans. Their extensive spatial coverage, fine temporal resolution, and inclusion of multiple variables make them particularly useful for impact assessments and attribution studies that extend beyond the capabilities of in-situ and satellite-based observations. This is especially important for snow variables, where both ground-based and remote sensing measurements are limited and face significant challenges, resulting in sparse and incomplete data. Having said that, reanalysis data are model-based; and therefore, their accuracy and reliability must be thoroughly evaluated before being applied in such studies. In this study, we focus on evaluating the snow variables of ERA5L, a high-resolution



land reanalysis dataset from the family of ECMWF reanalysis products. Our study targets the northern regions of North America, specifically Canada and Alaska, which are dominated by prolonged seasonal snow, in which snow variables are crucial areas for understanding hydrology, ecosystems, and regional climate. Although ERA5L snow fields have been previously assessed in other regions, we identify three key gaps in existing evaluations: (i) prior studies often overlook the scale mismatch between in-situ or remotely-sensed observations and the coarser reanalysis data; (ii) previous assessments have not explicitly analysed the ability of ERA5L to preserve spatial patterns in snow variables; and (iii) they have not examined whether there are spatial patterns in discrepancies that might indicate systematic biases in the reanalysis data. To address these gaps, we implement a rigorous and consistent benchmarking approach by evaluating ERA5L's SC, SD, and SWE against reference datasets, including MODIS's SC and CMC's SD/SWE products. Our analysis spans over 21 ecological regions of Canada and Alaska, covering monthly, seasonal, and annual scales to capture both temporal and spatial variability of discrepancies. By investigating the spatial and temporal patterns of these discrepancies, we aim to shed light on the potential biases in ERA5L's snow fields, and to provide insights into the quality and applicability of these reanalysis products for hydrological and water resources application.

For SC, our analysis reveals a tendency in ERA5L to overestimate the long-term mean, while underestimating both interannual variability and trends. We would like to reemphasize that the underestimation of trends refers also to instances where ERA5L reports stronger negative trends compared to reference datasets. These biases in the long-term mean and variability are more pronounced during the fall and spring. Discrepancies in trend estimates intensify during the fall and winter, and are particularly pronounced at monthly scales. Regarding SD and SWE, ERA5L constantly shows significant overestimations of the long-term mean and exhibit larger tendency for overestimating standard deviation. The degree of overestimation increases at the grid scale and is more pronounced during fall and spring. In contrast, ERA5L consistently underestimates trends in SD and SWE across all ecological regions, and this underestimation becomes more evident during the winter season and months. Despite these issues, ERA5L performs relatively well in terms of autocorrelation memory across the snow variables, showing good alignment with reference products in most ecological regions and across the various temporal scales considered. This suggests that ERA5L captures the temporal persistence of snow processes relatively well, particularly for SC, even though it struggles with accurately representing long-term means, interannual variability and trends.

At the annual scale, the spatial patterns of SC, SD, and SWE can be better preserved along latitudinal gradients. However, as the analysis shifts to seasonal and monthly scales, this alignment shifts toward elevation. Notably, spatial patterns of standard deviation, trends, and autocorrelation can be only preserved with respect to altitudinal gradients, regardless of the time scale considered. Our findings also reveal significant spatial patterns in the discrepancies between ERA5L and reference products. The spatial patterns of discrepancies are most pronounced along longitudinal gradients, particularly for SD, and become more significant when analysing the entire domain, rather than individual ecological regions, and are especially evident at monthly and seasonal scales.



Our study confirms the substantial overestimation of SWE and SD by ERA5L, consistent with recent findings in the literature (e.g., Kouki et al., 2023; Lei et al., 2023; Scherrer et al., 2023; Monteiro and Morin, 2023), which may be linked to the overestimation of snowfall (Orsolini et al., 2021). However, we go a step further by examining discrepancies in snow density estimates between ERA5L and the reference CMC product. Our results indicate that CMC's snow density estimates are generally higher, especially in northern ecological regions, at higher elevations, and during winter. While the discrepancies in trends of snow density between the two products can be notably large at the grid scale across all regions—with both overestimation and underestimation of CMC's snow density—these differences diminish significantly when aggregated at the ecological regions or across the entire domain. Additionally, we find that ERA5L exhibits a tendency to underestimate trends inferred by CMC's snow density at higher elevations, though this tendency is less pronounced than the tendency noted for long-term mean of snow density.

Our findings highlight key discrepancies between ERA5L and reference products across Canada and Alaska. Based on our analysis, we conclude that ERA5L's estimates of SD and SWE are less reliable than its SC field. Considering the entire domain and during the whole study period, the average SWE is estimated by CMC as 85.4 mm, but 306.9 mm by ERA5L. Accordingly, we advise against using SD and SWE directly for impact assessment and attribution studies in Canada and Alaska. However, we also observe that the discrepancies in SWE are primarily driven by errors in SD rather than snow density. As such, we believe ERA5L's estimates of SC and snow density can still be utilized in Canada and Alaska, albeit with caution. For localized studies, we recommend bias-correcting ERA5L's SC and snow density using in-situ and satellite observations. At larger regional scales, spatial bias correction should also be considered. Additionally, ERA5L's SC and snow density estimates could be integrated with more reliable SD products to produce improved gridded estimates of SWE and regional snow water availability.

We hope our study fosters more informed and effective use of ERA5L reanalysis data for snow-related research in the Great White North.

### Data availability

All data used in this study are publicly available. ERA5-Land data can be obtained at Climate Data Store, available at <https://cds.climate.copernicus.eu/datasets/reanalysis-era5-land?tab=download>. CMC's SD/SWE product is available at NASA's NSIDC available at <https://nsidc.org/data/nsidc-0447/versions/1#anchor-data-access-tools>. MODIS data can be also obtained from NASA's NSIDC at <https://nsidc.org/data/mod10cm/versions/61#anchor-documentation>. Elevation data can be obtained from USGS available at <https://www.usgs.gov/coastal-changes-and-impacts/gmted2010>.

### Supplement

There is Supplement file associated with this manuscript that is submitted along with the paper for peer review.



## Competing interests

595 Authors do not have any competing interests.

## Acknowledgments

Financial support of this research is provided by Canada's New Frontier Research Fund Exploration stream (NFRFE-2020-01298). To the memory of Fariborz Vaziri, Iran's premier glaciologist.

## References

- 600 Akyurek, Z., Kuter, S., Karaman, Ç. H., and Akpınar, B.: Understanding the snow cover climatology over Turkey from ERA5-Land reanalysis data and MODIS snow cover frequency product, *Geosci.*, 13, 311, <https://doi.org/10.3390/geosciences13100311>, 2023.
- Amatulli, G., Domisch, S., Tuanmu, M. N., Parmentier, B., Ranipeta, A., Malczyk, J., and Jetz, W.: A suite of global, cross-scale topographic variables for environmental and biodiversity modeling, *Sci. Data*, 5, 180040, <https://doi.org/10.1038/sdata.2018.40>, 2018.
- 605 Amir Jabbari, A. and Nazemi, A.: Alterations in Canadian hydropower production potential due to continuation of historical trends in climate variables, *Resources*, 8, 163, <https://doi.org/10.3390/resources8040163>, 2019.
- Appel, I.: Uncertainty in satellite remote sensing of snow fraction for water resources management, *Front. Earth Sci.*, 12, 711–727, <https://doi.org/10.1007/s11707-018-0726-x>, 2018.
- 610 Bair, E. H., Rittger, K., Davis, R. E., Painter, T. H., and Dozier, J.: Validating reconstruction of snow water equivalent in California's Sierra Nevada using measurements from the NASA Airborne Snow Observatory, *Water Resour. Res.*, 52, 8437–8460, <https://doi.org/10.1002/2016WR018704>, 2016.
- Balsamo, G., Viterbo, P., Beljaars, A., van den Hurk, B., Hirschi, M., Betts, A. K., and Scipal, K.: A revised hydrology for the ECMWF model: Verification from field site to terrestrial water storage and impact in the Integrated Forecast System, *J. Hydrometeorol.*, 10, 623–643, <https://doi.org/10.1175/2008JHM1068.1>, 2009.
- 615 Barnett, T. P., Adam, J. C., and Lettenmaier, D. P.: Potential impacts of a warming climate on water availability in snow-dominated regions, *Nature*, 438, 303–309, <https://doi.org/10.1038/nature04141>, 2005.
- Baxter, R., Clelland, A., and Marshall, G.: Evaluating the performance of key ERA-Interim, ERA5, and ERA5-Land climate variables across Siberia, *Int. J. Climatol.*, 44, 2318–2342, <https://doi.org/10.1002/joc.8456>, 2024.
- 620 Bitz, C. M., and Battisti, D. S.: Interannual to decadal variability in climate and the glacier mass balance in Washington, western Canada, and Alaska, *J. Climate*, 12, 3181–3196, [https://doi.org/10.1175/1520-0442\(1999\)012<3181:ITDVIC>2.0.CO;2](https://doi.org/10.1175/1520-0442(1999)012<3181:ITDVIC>2.0.CO;2), 1999.



- Boelman, N. T., Liston, G. E., Gurarie, E., Meddens, A. J., Mahoney, P. J., Kirchner, P. B., ... and Vierling, L. A.: Integrating snow science and wildlife ecology in Arctic-boreal North America, *Environ. Res. Lett.*, 14, 010401, <https://doi.org/10.1088/1748-9326/aaf9a9>, 2019.
- Bormann, K. J., Westra, S., Evans, J. P., and McCabe, M. F.: Spatial and temporal variability in seasonal snow density, *J. Hydrol.*, 484, 63–73, <https://doi.org/10.1016/j.jhydrol.2013.01.032>, 2013.
- Brown, R. D. and Frei, A.: Comment on “Evaluation of surface albedo and snow cover in AR4 coupled models” by A. Roesch, *J. Geophys. Res.-Atmos.*, 112, D22, <https://doi.org/10.1029/2007JD008480>, 2007.
- Brown, R. D., Brasnett, B., and Robinson, D.: Gridded North American monthly snow depth and snow water equivalent for GCM evaluation, *Atmos.-Ocean*, 41, 1–14, <https://doi.org/10.3137/ao.410101>, 2003.
- Brown, R. D., Smith, C., Derksen, C., and Mudryk, L.: Canadian in situ snow cover trends for 1955–2017 including an assessment of the impact of automation, *Atmos.-Ocean*, 59, 77–92, <https://doi.org/10.1080/07055900.2021.1915450>, 2021.
- Broxton, P. D. and van Leeuwen, W. J. D.: Structure from motion of multi-angle RPAS imagery complements larger-scale airborne lidar data for cost-effective snow monitoring in mountain forests, *Remote Sens.*, 12, 2311, <https://doi.org/10.3390/rs12142311>, 2020.
- Brubaker, K. L., Pinker, R. T., and Deviatova, E.: Evaluation and comparison of MODIS and IMS snow-cover estimates for the continental United States using station data, *J. Hydrometeorol.*, 6, 1002–1017, <https://doi.org/10.1175/JHM462.1>, 2005.
- Byun, K. and Choi, M.: Uncertainty of snow water equivalent retrieved from AMSR-E brightness temperature in northeast Asia, *Hydrol. Process.*, 28, 3173–3184, <https://doi.org/10.1002/hyp.9833>, 2014.
- Callaghan, T. V., Johansson, M., Brown, R. D., Groisman, P. Y., Labba, N., Radionov, V., et al.: Multiple effects of changes in Arctic snow cover, *Ambio*, 40, 32–45, <https://doi.org/10.1007/s13280-011-0212-x>, 2011.
- Danielson, J. J. and Gesch, D. B.: Global multi-resolution terrain elevation data 2010 (GMTED2010), US Geol. Surv. Open-File Rep., 2011-1073, <https://doi.org/10.3133/ofr20111073>, 2011.
- DeBeer, C. M., Wheeler, H. S., Carey, S. K., and Chun, K. P.: Recent climatic, cryospheric, and hydrological changes over the interior of western Canada: a review and synthesis, *Hydrol. Earth Syst. Sci.*, 20, 1573–1598, <https://doi.org/10.5194/hess-20-1573-2016>, 2016.
- Deems, J. S., Painter, T. H., and Finnegan, D. C.: Lidar measurement of snow depth: a review, *J. Glaciol.*, 59, 467–479, <https://doi.org/10.3189/2013JoG12J145>, 2013.
- Deng, H., Chen, Y., and Li, Y.: Glacier and snow variations and their impacts on regional water resources in mountains, *J. Geogr. Sci.*, 29, 84–100, <https://doi.org/10.1007/s11442-019-1585-2>, 2019.
- Di Marco, N., Avesani, D., Righetti, M., Zaramella, M., Majone, B., and Borga, M.: Reducing hydrological modelling uncertainty by using MODIS snow cover data and a topography-based distribution function snowmelt model, *J. Hydrol.*, 599, 126020, <https://doi.org/10.1016/j.jhydrol.2021.126020>, 2021.
- Dietz, A. J., Kuenzer, C., Gessner, U., and Dech, S.: Remote sensing of snow—a review of available methods, *Int. J. Remote Sens.*, 33, 4094–4134, <https://doi.org/10.1080/01431161.2012.669570>, 2012.



- Dong, C.: Remote sensing, hydrological modeling, and in situ observations in snow cover research: A review, *J. Hydrol.*, 561, 573–583, <https://doi.org/10.1016/j.jhydrol.2018.04.024>, 2018.
- Dong, J., Walker, J. P., and Houser, P. R.: Factors affecting remotely sensed snow water equivalent uncertainty, *Remote Sens. Environ.*, 97, 68–82, <https://doi.org/10.1016/j.rse.2005.03.019>, 2005.
- Ermolaev, O. P., Mal'tsev, K. A., Mukharamova, S. S., Kharchenko, S. V., and Vedeneva, E. A.: Cartographic model of river basins of European Russia, *Geogr. Nat. Res.*, 38, 131–138, 2017.
- Fang, Y., and Leung, L. R.: Northern Hemisphere Snow Drought in Earth System Model Simulations and ERA5-Land Data in 1980–2014, *J. Geophys. Res.: Atmos.*, 128, e2023JD039308, <https://doi.org/10.1029/2023JD039308>, 2023.
- 665 Fatolahzadeh Gheysari, A., Maghoul, P., Ojo, E. R., and Shalaby, A.: Reliability of ERA5 and ERA5-Land reanalysis data in the Canadian Prairies, *Theor. Appl. Climatol.*, 155, 3087–3098, <https://doi.org/10.1007/s00704-024-03912-0> 2024.
- Foster, J. L., Sun, C., Walker, J. P., Kelly, R., Chang, A., Dong, J., and Powell, H.: Quantifying the uncertainty in passive microwave snow water equivalent observations, *Remote Sens. Environ.*, 94, 187–203, <https://doi.org/10.1016/j.rse.2004.09.004>, 2005.
- 670 Frei, A., Brown, R., Miller, J. A., and Robinson, D. A.: Snow mass over North America: Observations and results from the second phase of the atmospheric model intercomparison project, *J. Hydrometeorol.*, 6, 681–695, <https://doi.org/10.1175/JHM446.1>, 2005.
- Gao, S., Li, Z., Zhang, P., Zeng, J., Chen, Q., Zhao, C., et al.: An assessment of the applicability of three reanalysis snow density datasets over China using ground observations, *IEEE Geosci. Remote Sens. Lett.*, 19, 1–5, <https://doi.org/10.1109/LGRS.2021.3068233>, 2022.
- 675 Gleason, K. E., and Nolin, A. W.: Charred forests accelerate snow albedo decay: Parameterizing the post-fire radiative forcing on snow for three years following fire, *Hydrol. Process.*, 30, 3855–3870, <https://doi.org/10.1002/hyp.10999>, 2016.
- Graham, R. M., Cohen, L., Ritzhaupt, N., Segger, B., Graversen, R. G., Rinke, A., Walden, V. P., Granskog, M. A., and Hudson, S. R.: Evaluation of six atmospheric reanalyses over Arctic sea ice from winter to early summer, *J. Clim.*, 32, 4121–4143, <https://doi.org/10.1175/JCLI-D-18-0643.1>, 2019.
- 680 Grody, N. C., and Basist, A. N.: Global identification of snowcover using SSM/I measurements, *IEEE Trans. Geosci. Remote Sens.*, 34, 237–249, <https://doi.org/10.1109/36.485512>, 1996.
- Hall, D. K., and Riggs, G. A.: Accuracy assessment of the MODIS snow products, *Hydrol. Process.*, 21, 1534–1547, <https://doi.org/10.1002/hyp.6715>, 2007.
- 685 Hall, D. K., Foster, J. L., Verbyla, D. L., Klein, A. G., and Benson, C. S.: Assessment of snow-cover mapping accuracy in a variety of vegetation-cover densities in central Alaska, *Remote Sens. Environ.*, 66, 129–137, [https://doi.org/10.1016/S0034-4257\(98\)00032-7](https://doi.org/10.1016/S0034-4257(98)00032-7), 1998.
- Hall, D. K., Riggs, G. A., Salomonson, V. V., DiGirolamo, N. E., and Bayr, K. J.: MODIS snow-cover products, *Remote Sens. Environ.*, 83, 181–194, [https://doi.org/10.1016/S0034-4257\(02\)00008-8](https://doi.org/10.1016/S0034-4257(02)00008-8), 2002.



- 690 Hamm, A., Arndt, A., Kolbe, C., Wang, X., Thies, B., Boyko, O., et al.: Intercomparison of gridded precipitation datasets over a sub-region of the Central Himalaya and the Southwestern Tibetan Plateau, *Water*, 12, 3271, <https://doi.org/10.3390/w12113271>, 2020.
- Hassler, B., and Lauer, A.: Comparison of reanalysis and observational precipitation datasets including ERA5 and WFDE5, *Atmosphere*, 12, 1462, <https://doi.org/10.3390/atmos12111462>, 2021.
- 695 Hatami, S., and Nazemi, A.: A statistical framework for assessing temperature controls on landscape freeze-thaw: Application and implications in Québec, Canada (1979–2016), *J. Hydrol.*, 603, 126891, <https://doi.org/10.1016/j.jhydrol.2021.126891>, 2021.
- Hatami, S., and Nazemi, A.: Compound changes in temperature and snow depth lead to asymmetric and nonlinear responses in landscape freeze-thaw, *Sci. Rep.*, 12, 2196, <https://doi.org/10.1038/s41598-022-09071-4>, 2022.
- 700 Henn, B., Newman, A. J., Livneh, B., Daly, C., and Lundquist, J. D.: An assessment of differences in gridded precipitation datasets in complex terrain, *J. Hydrol.*, 556, 1205–1219, <https://doi.org/10.1016/j.jhydrol.2017.03.008>, 2018.
- Hersbach, H., Bell, B., Berrisford, P., Hirahara, S., Horányi, A., Muñoz-Sabater, J., et al.: The ERA5 global reanalysis, *Q. J. Roy. Meteor. Soc.*, 146, 1999–2049, <https://doi.org/10.1002/qj.3803>, 2020.
- Huning, L. S., and AghaKouchak, A.: Global snow drought hot spots and characteristics, *Proc. Natl. Acad. Sci.*, 117, 19753–
- 705 19759, <https://doi.org/10.1073/pnas.2007565117>, 2020.
- Kaemo, M., Hassanzadeh, E., and Nazemi, A.: A locally relevant framework for assessing the risk of sea level rise under changing temperature conditions: Application in New Caledonia, Pacific Ocean, *Sci. Total Environ.*, 834, 155326, <https://doi.org/10.1016/j.scitotenv.2022.155326>, 2022.
- Kazama, S., Izumi, H., Sarukkalgige, P. R., Nasu, T., and Sawamoto, M.: Estimating snow distribution over a large area and its
- 710 application for water resources, *Hydrol. Process.*, 22, 2315–2324, <https://doi.org/10.1002/hyp.7008>, 2008.
- Kelly, R. E., Chang, A. T., Tsang, L., and Foster, J. L.: A prototype AMSR-E global snow area and snow depth algorithm, *IEEE Trans. Geosci. Remote Sens.*, 41, 230–242, <https://doi.org/10.1109/TGRS.2002.808598>, 2003.
- Kim, Y., Kimball, J. S., Du, J., Schaaf, C. L. B., and Kirchner, P. B.: Quantifying the effects of freeze-thaw transitions and snowpack melt on land surface albedo and energy exchange over Alaska and Western Canada, *Environ. Res. Lett.*, 13, 074028,
- 715 <https://doi.org/10.1088/1748-9326/aacf72>, 2018.
- Kim, Y., Kimball, J. S., Glassy, J., and Du, J.: An extended global Earth system data record on daily landscape freeze–thaw status determined from satellite passive microwave remote sensing, *Earth Syst. Sci. Data*, 9, 133–147, <https://doi.org/10.5194/essd-9-133-2017>, 2017.
- Kouki, K., Luojus, K., and Riihelä, A.: Evaluation of snow cover properties in ERA5 and ERA5-Land with several satellite-
- 720 based datasets in the Northern Hemisphere in spring 1982–2018, *The Cryosphere Discuss.*, 2023, 1–33, <https://doi.org/10.5194/tc-2023-1>, 2023.
- Kusch, E., and Davy, R.: KrigR—a tool for downloading and statistically downscaling climate reanalysis data, *Environ. Res. Lett.*, 17, 024005, <https://doi.org/10.1088/1748-9326/ac42f4>, 2022.



- Lackner, G., Domine, F., Nadeau, D. F., Parent, A.-C., Anctil, F., Lafaysse, M., and Dumont, M.: On the energy budget of a low-Arctic snowpack, *The Cryosphere*, 16, 127–142, <https://doi.org/10.5194/tc-2021-255>, 2022.
- Lehning, M.: Snow–atmosphere interactions and hydrological consequences, *Adv. Water Resour.*, 55, 1–3, <https://doi.org/10.1016/j.advwatres.2012.04.008>, 2013.
- Lei, Y., Pan, J., Xiong, C., Jiang, L., and Shi, J.: Snow depth and snow cover over the Tibetan Plateau observed from space in comparison with ERA5: Matters of scale, *Clim. Dyn.*, 60, 1523–1541, <https://doi.org/10.1007/s00382-022-06062-x>, 2023.
- Li, H., Wang, Z., He, G., and Man, W.: Estimating snow depth and snow water equivalence using repeat-pass interferometric SAR in the northern piedmont region of the Tianshan Mountains, *J. Sens.*, 2017, 8739598, <https://doi.org/10.1155/2017/8739598>, 2017.
- Lindsay, R., Wensnahan, M., Schweiger, A., and Zhang, J.: Evaluation of seven different atmospheric reanalysis products in the Arctic, *J. Clim.*, 27, 2588–2606, <https://doi.org/10.1175/JCLI-D-13-00477.1>, 2014.
- Ma, H., Zhang, G., Mao, R., Su, B., Liu, W., and Shi, P.: Snow depth variability across the Qinghai Plateau and its influencing factors during 1980–2018, *Int. J. Climatol.*, 43, 1094–1111, <https://doi.org/10.1002/joc.7883>, 2023.
- Marshall, H. P., and Koh, G.: FMCW radars for snow research, *Cold Reg. Sci. Technol.*, 52, 118–131, <https://doi.org/10.1016/j.coldregions.2007.03.001>, 2008.
- Maurer, E. P., Rhoads, J. D., Dubayah, R. O., and Lettenmaier, D. P.: Evaluation of the snow-covered area data product from MODIS, *Hydrol. Process.*, 17, 59–71, <https://doi.org/10.1002/hyp.787>, 2003.
- McMahon, G., Wiken, E. B., and Gauthier, D. A.: Toward a scientifically rigorous basis for developing mapped ecological regions, *Environ. Manage.*, 34, S111–S124, <https://doi.org/10.1007/s00267-004-5017-9>, 2004.
- Mitterer, C., and Schweizer, J.: Analysis of the snow-atmosphere energy balance during wet-snow instabilities and implications for avalanche prediction, *The Cryosphere*, 7, 205–216, <https://doi.org/10.5194/tc-7-205-2013>, 2013.
- Molotch, N. P., Fassnacht, S. R., Bales, R. C., and Helfrich, S. R.: Estimating the distribution of snow water equivalent and snow extent beneath cloud cover in the Salt-Verde River basin, Arizona, *Hydrol. Process.*, 18, 1595–1611, <https://doi.org/10.1002/hyp.1408>, 2004.
- Monteiro, D., and Morin, S.: Multi-decadal analysis of past winter temperature, precipitation, and snow cover data in the European Alps from reanalyses, climate models, and observational datasets, *The Cryosphere*, 17, 3617–3660, <https://doi.org/10.5194/tc-17-3617-2023>, 2023.
- Morice, C. P., Kennedy, J. J., Rayner, N. A., and Jones, P. D.: Quantifying uncertainties in global and regional temperature change using an ensemble of observational estimates: The HadCRUT4 data set, *J. Geophys. Res. Atmos.*, 117, D08101, <https://doi.org/10.1029/2011JD017187>, 2012.
- Muñoz-Sabater, J., Dutra, E., Agustí-Panareda, A., Albergel, C., Arduini, G., Balsamo, G., and Thépaut, J. N.: ERA5-Land: A state-of-the-art global reanalysis dataset for land applications, *Earth Syst. Sci. Data*, 13, 4349–4383, <https://doi.org/10.5194/essd-13-4349-2021>, 2021.



- Musselman, K. N., Addor, N., Vano, J. A., and Molotch, N. P.: Winter melt trends portend widespread declines in snow water resources, *Nat. Clim. Change*, 11, 418–424, <https://doi.org/10.1038/s41558-021-01014-9>, 2021.
- Nazemi, A., Wheeler, H. S., Chun, K. P., Bonsal, B., and Mekonnen, M.: Forms and drivers of annual streamflow variability in the headwaters of Canadian Prairies during the 20th century, *Hydrol. Process.*, 31, 221–239, <https://doi.org/10.1002/hyp.10927>, 2017.
- Niu, G. Y., and Yang, Z. L.: An observation-based formulation of snow cover fraction and its evaluation over large North American river basins, *J. Geophys. Res. Atmos.*, 112, D21106, <https://doi.org/10.1029/2007JD008674>, 2007.
- Omernik, J. M., and Griffith, G. E.: Ecoregions of the conterminous United States: evolution of a hierarchical spatial framework, *Environ. Manage.*, 54, 1249–1266, <https://doi.org/10.1007/s00267-014-0367-4>, 2014.
- Omernik, J. M.: Perspectives on the nature and definition of ecological regions, *Environ. Manage.*, 34, S27–S38, <https://doi.org/10.1007/s00267-004-5009-x>, 2004.
- Orsolini, Y., Wegmann, M., Dutra, E., Liu, B., Balsamo, G., Yang, K., and Arduini, G.: Evaluation of snow depth and snow cover over the Tibetan Plateau in global reanalyses using in situ and satellite remote sensing observations, *The Cryosphere*, 13, 2221–2239, <https://doi.org/10.5194/tc-13-2221-2019>, 2019.
- Pakoksung, K., and Takagi, M.: Effect of DEM sources on distributed hydrological model to results of runoff and inundation area, *Model. Earth Syst. Environ.*, 7, 1891–1905, <https://doi.org/10.1007/s40808-021-01267-2>, 2021.
- Parajka, J., and Blöschl, G.: The value of MODIS snow cover data in validating and calibrating conceptual hydrologic models, *J. Hydrol.*, 358, 240–258, <https://doi.org/10.1016/j.jhydrol.2008.06.003>, 2008.
- Rapaić, M., Brown, R., Markovic, M., and Chaumont, D.: An evaluation of temperature and precipitation surface-based and reanalysis datasets for the Canadian Arctic, 1950–2010, *Atmos. Ocean*, 53, 283–303, <https://doi.org/10.1080/07055900.2015.1035962>, 2015.
- Saavedra, F. A., Kampf, S. K., Fassnacht, S. R., and Sibold, J. S.: Changes in Andes snow cover from MODIS data, 2000–2016, *The Cryosphere*, 12, 1027–1046, <https://doi.org/10.5194/tc-12-1027-2018>, 2018.
- Scherrer, S. C., Göldi, M., Gubler, S., Steger, C. R., and Kotlarski, S.: Towards a spatial snow climatology for Switzerland: Comparison and validation of existing datasets, *Meteorol. Z.*, 33, 101–116, <https://doi.org/10.1127/metz/2023/1298>, 2023.
- Schilling, S., Dietz, A., and Kuenzer, C.: Snow Water Equivalent Monitoring—A Review of Large-Scale Remote Sensing Applications, *Remote Sens.*, 16, 1085, <https://doi.org/10.3390/rs16061085>, 2024.
- Schumacher, V., Justino, F., Fernández, A., Meseguer-Ruiz, O., Sarricolea, P., Comin, A., Peroni Venancio, L., and Althoff, D.: Comparison between observations and gridded data sets over complex terrain in the Chilean Andes: Precipitation and temperature, *Int. J. Climatol.*, 40, 5266–5288, <https://doi.org/10.1002/joc.6518>, 2020.
- Sexstone, G. A., Clow, D. W., Stannard, D. I., and Fassnacht, S. R.: Comparison of methods for quantifying surface sublimation over seasonally snow-covered terrain, *Hydrol. Process.*, 30, 3373–3389, <https://doi.org/10.1002/hyp.10864>, 2016.



- 790 Shijin, W., Yuande, Y., and Yanjun, C.: Global snow-and ice-related disaster risk: A review, *Nat. Hazards Rev.*, 23, 03122002, <https://doi.org/10.1061/NHREAY.0000253>, 2022.
- Skaugen, T., Stranden, H. B., and Saloranta, T.: Trends in snow water equivalent in Norway (1931–2009), *Hydrol. Res.*, 43, 489–499, <https://doi.org/10.2166/nh.2012.009>, 2012.
- Stähli, M., Stacheder, M., Gustafsson, D., Schlaeger, S., Schneebeli, M., and Brandelik, A.: A new in situ sensor for large-  
 795 scale snow-cover monitoring, *Ann. Glaciol.*, 38, 273–278, <https://doi.org/10.3189/172756404781813631>, 2004.
- Stiegler, C., Lund, M., Christensen, T. R., Mastepanov, M., and Lindroth, A.: Effects of interannual variability in snow accumulation on energy partitioning and surface energy exchange in a high-Arctic tundra ecosystem, *The Cryosphere Discuss.*, <https://doi.org/10.5194/tc-2016-5>, 2016.
- Sturm, M., Taras, B., Liston, G. E., Derksen, C., Jonas, T., and Lea, J.: Estimating snow water equivalent using snow depth  
 800 data and climate classes, *J. Hydrometeorol.*, 11, 1380–1394, <https://doi.org/10.1175/2010JHM1202.1>, 2010.
- Sun, Q., Miao, C., Duan, Q., Ashouri, H., Sorooshian, S., and Hsu, K. L.: A review of global precipitation data sets: Data sources, estimation, and intercomparisons, *Rev. Geophys.*, 56, 79–107, <https://doi.org/10.1002/2017RG000574>, 2018.
- Trepte, Q., Minnis, P., and Arduini, R. F.: Daytime and nighttime polar cloud and snow identification using MODIS data, in *Optical Remote Sensing of the Atmosphere and Clouds III*, vol. 4891, SPIE, 449–459, <https://doi.org/10.1117/12.468374>,  
 805 2003.
- Vionnet, V., Mortimer, C., Brady, M., Arnal, L., and Brown, R.: Canadian historical snow water equivalent dataset (CanSWE, 1928–2020), *Earth Syst. Sci. Data*, 13, 4603–4619, <https://doi.org/10.5194/essd-13-4603-2021>, 2021.
- Wang, Y., and Zheng, Z.: Spatial representativeness analysis for snow depth measurements of meteorological stations in northeast China, *J. Hydrometeorol.*, 21, 791–805, <https://doi.org/10.1175/JHM-D-19-0134.1>, 2020.
- 810 Willeit, M., and Ganopolski, A.: The importance of snow albedo for ice sheet evolution over the last glacial cycle, *Clim. Past*, 14, 697–707, <https://doi.org/10.5194/cp-2017-122>, 2018.
- Wright, R. G., Murray, M. P., and Merrill, T.: Ecoregions as a level of ecological analysis, *Biol. Conserv.*, 86, 207–213, [https://doi.org/10.1016/S0006-3207\(97\)00057-4](https://doi.org/10.1016/S0006-3207(97)00057-4), 1998.
- Xu, J., Ma, Z., Yan, S., and Peng, J.: Do ERA5 and ERA5-land precipitation estimates outperform satellite-based precipitation  
 815 products? A comprehensive comparison between state-of-the-art model-based and satellite-based precipitation products over mainland China, *J. Hydrol.*, 605, 127353, <https://doi.org/10.1016/j.jhydrol.2021.127353>, 2022.
- Yoon, Y., Kemp, E. M., Kumar, S. V., Wegiel, J. W., Vuyovich, C. M., and Peters-Lidard, C.: Development of a global operational snow analysis: The US Air Force Snow and Ice Analysis, *Remote Sens. Environ.*, 278, 113080, <https://doi.org/10.1016/j.rse.2022.113080>, 2022.
- 820 You, J., Tarboton, D. G., and Luce, C. H.: Modeling the snow surface temperature with a one-layer energy balance snowmelt model, *Hydrol. Earth Syst. Sci.*, 18, 5061–5076, <https://doi.org/10.5194/hess-18-5061-2014>, 2014.



Zaerpour, M., Hatami, S., Sadri, J., and Nazemi, A.: A global algorithm for identifying changing streamflow regimes: Application to Canadian natural streams (1966–2010), *Hydrol. Earth Syst. Sci.*, 25, 5193–5217, <https://doi.org/10.5194/hess-25-5193-2021>, 2021a.

825 Zaerpour, M., Papalexiou, S. M., and Nazemi, A.: Informing stochastic streamflow generation by large-scale climate indices at single and multiple sites, *Adv. Water Resour.*, 156, 104037, <https://doi.org/10.1016/j.advwatres.2021.104037>, 2021b.